Dynamics and Energy Extraction of a Surging and Plunging Airfoil at Low Reynolds Number

Jeesoon Choi* and Tim Colonius†
California Institute of Technology, Pasadena, CA 91125, USA
David Williams‡
Illinois Institute of Technology, Chicago, IL 60616, USA

We investigate the unsteady aerodynamic forces and energy transfer associated with harmonic surging (streamwise) and plunging (transverse) motion of a thin airfoil at low Reynolds number. Two-dimensional unsteady flows are simulated over a large range of amplitude and reduced-frequency of the oscillatory motion using the immersed boundary projection method, and the computational results are compared to inviscid flow models and experiments. At low angle of attack there is reasonable agreement with inviscid theory for the amplitude and phase of lift fluctuations, despite the low Reynolds number. At high angle of attack, the separated flow leads to larger lift and drag fluctuations not captured by inviscid models. At frequencies below the vortex shedding frequency, lift fluctuations are first enhanced and then attenuated depending on the phase between the freestream velocity and the forming leading-edge vortex. Resonance with the vortex shedding frequency also occurs. The time-averaged forces and power supplied by the oscillating airfoil are also evaluated to find frequency ranges that are favorable for the airfoil.

Nomenclature

A	peak-to-peak amplitude of unsteady airfoil motion
c	airfoil chord length
C_D	drag coefficient
C_L	lift coefficient
k	reduced frequency, $(\pi f c/U)$
k_{vs}	reduced frequency corresponding to vortex shedding
$k_{\text{vs, crit}}$	reduced frequency corresponding to vortex shedding at Re_{crit}
L_{am}	added mass lift
L_{qs}	quasi-steady lift
L_{wake}	lift induced by vorticity distribution of wake
L_0	mean lift at a constant velocity
$\bar{L}$	mean lift
$\hat{L}_k$	magnitude of Fourier coefficient of lift at frequency k
P	power per unit mass
Re	Reynolds Number, (cU/ν)
Re_{crit}	Critical Reynolds Number
St_A	Strouhal number scaled with peak-to-peak amplitude (fA/U)
T	period
u	streamwise airfoil velocity
U	reference velocity

*Graduate Student, Mechanical Engineering, Student Member AIAA
†Professor, Mechanical Engineering, Associate Fellow AIAA
‡Professor, Mechanical and Aerospace Engineering , Associate Fellow AIAA

v	transverse airfoil velocity
α	angle of attack
ν	fluid kinematic viscosity
ρ	fluid density
σ_x	dimensionless amplitude of oscillating streamwise velocity
σ_y	dimensionless amplitude of oscillating transverse velocity
ϕ	phase of lift leading velocity
Γ	circulation
DVM	Discrete Vortex Model
LEV	Leading Edge Vortex

I. Introduction

Conventional models of aerodynamic forces for flight control rely on a quasi-steady assumption where the aerodynamic forces depend on the instantaneous state of the flow through a static map. When the flow varies rapidly, classical inviscid potential-flow models account for unsteadiness through added mass and trailing-edge Kutta condition that leads to an unsteady distribution of vorticity in the wake.[1–3] The behavior of lift at low angle of attack (α) is, by and large, well described by these models. However, at higher values of α that can be relevant for the motion and gust response of micro air vehicles,[4–6] the flow separates at the leading edge, and inviscid theories no longer provide a useful prediction.

Stalled flow at high α involves rapid fluctuations in lift and drag and is unsuitable for fixed-wing aircraft at high Reynolds number. However, for small insects and birds that fly at relatively low Reynolds number, the unsteady motion (flapping) produces much higher lift than the steady case.[7–9] The low-pressure region produced by the leading-edge vortex (LEV) has been invoked to explain this phenomenon. A number of studies have focused on the behavior of the aerodynamics forces at high angles of attack, and suggest that optimal frequencies exist for flying or swimming.[7,10–12] For example, by experimentally measuring the thrust generated by an oscillating airfoil, Triantafyllou *et al.*[11] has reported this value to be $0.25 < St_A < 0.35$ (St_A is the Strouhal number scaled with the peak-to-peak oscillating amplitude of the trailing edge), and Taylor *et al.*[10] suggest $0.20 < St_A < 0.40$ by comparing a variety of animals from insects to dolphins.

Energy transfer between the airfoil and the surrounding fluids will also be influenced by the unsteady motion of the airfoil and spatio-temporal fluctuations in the wind. Unsteady flow structures alter the phase and magnitude of the aerodynamic forces and the amount of power required for flight (possibly negative!) will be highly dependent on airfoil's specific motion and the wake dynamics. Williams, *et al.*[13] have shown that combining vertical motions of an airfoil with a streamwise oscillating gust, the net energy gain of the airfoil could be positive when the lift and drag fluctuations are large enough.

In this paper, we consider the forces induced by harmonic airfoil motion in the streamwise (surging) and transverse (plunging) directions. These forces are essentially equivalent, for a thin airfoil in air, to those on a fixed airfoil in an unsteady stream with streamwise and transverse fluctuations. We restrict our attention to two-dimensional flow at Reynolds numbers, $Re = O(10^2)$, where, depending on α, we may have subcritical, steady flow or supercritical, unsteady flow with wake instability. This allows us to isolate the effect of wake instability from the response to unsteady motion, even when their frequencies are similar. We understand that even for an infinite aspect-ratio wing, the two-dimensional flow assumption is not adequate to describe the transition of the wake that would likely occur at some of the super-critical values of Re we consider. However, a complete description of the bifurcations to three-dimensional flow in this geometry, especially in unsteady flow, is lacking and, despite the simplifications, there is qualitative agreement between our results and experiments at much higher Re.

We consider a range of amplitudes and reduced frequencies of surging and plunging, from zero to beyond the frequency associated with wake instability (vortex shedding). Since, most of the past work related to unsteady airfoil motion were focused on plunging,[14–18] surging is considered here in greater detail. In the next section, we briefly discuss the numerical method, the problem setup, and comparative inviscid models

appropriate for unsteady flow at low α. The results are given in section III, where we highlight the role played by the forming leading-edge vortex in force production. Conclusions and directions for future research are given in section IV.

II. Preliminaries

A. Numerical method

Two dimensional incompressible flows are computed in an airfoil-fixed reference frame using the immersed boundary (IB) projection method.[19,20] The method solves for a discrete streamfunction on multiple overlapping and progressively coarser grids. Five grid levels are used for the present computations; each level has the same number of grid points (240×160), and the coarsest grid extends to 32 and 48 chord lengths in the transverse and streamwise directions, respectively. Convergence tests performed on 480×320 and 960×640 grids showed that the 240×160 resolution was sufficient. The time step was $\Delta tU/c = 0.0025$ for most of the cases.

Airfoils with oscillatory motion are solved in the (non-inertial) reference frame of the body. It was deemed sufficient to compute about 10 periods of oscillation to remove transients associated with the startup of oscillatory motion, after which an additional 10 periods of steady-state oscillation were computed to determine the fluctuating forces via the Fourier transform, and correlations to determine their phase with respect to the imposed sinusoidal motion.

B. Airfoil and motion

In the simulations, two different airfoils were initially considered: a thin flat plate and a NACA 0006. The flat plate is idealized as infinitely thin, but the IB method regularizes the thickness with the grid spacing. The lift response was substantially the same for both airfoils and in what follows, we only present results for the thin flat plate.

The x and y components of the motion of the body are specified as

$$u = U\left(1 + \sigma_x \sin\left(2ktU/c\right)\right), \tag{1}$$

$$v = U\sigma_y \sin\left(2ktU/c + \theta\right), \tag{2}$$

where k is the reduced frequency, $U\sigma_x$ and $U\sigma_y$ are the fluctuating velocities in the x (streamwise, surging) and y (transverse, plunging) directions, respectively, and θ is the phase between plunge and surge. In this paper, we only consider plunge and surge independently, so θ is not used. We note that when (typically plunging) motions are characterized by a peak-to-peak displacement, A, then the quantity St_A is related to σ by $St_A = \frac{\sigma}{\pi}$.

This unsteady airfoil motion can, in the present case, be reinterpreted as a temporally varying freestream velocity, representing a uniform stream with an oscillatory gust in the streamwise and transverse directions. This is because the apparent buoyancy force, $\rho\dot{\mathbf{u}}V_b$, where V_b is the volume of the body, is negligible for a thin airfoil in air for the range of reduced frequencies considered here.

For simplicity, in what follows we refer to drag and lift as the forces in the $-x$ and $+y$ directions, respectively. For the plunging case ($\sigma_y \neq 0$), what we term the lift force is therefore not instantaneously normal to the freestream.

C. Wake instability in steady motion

We consider first steady motion ($\sigma_x = \sigma_y = 0$) to determine the critical Reynolds, Re_{crit}, number beyond which there is wake instability, and to characterize the resulting natural frequency of vortex shedding, $k_{\text{vs, crit}}$. The results are shown in Figure 1 for different angles of attack. Also plotted are the Reynolds numbers and reduced frequencies based on the *projected chord length*, $c\sin\alpha$, as their length scale. This

gives a nearly constant frequency of vortex shedding[21] which corresponds to a Strouhal number of 0.13. The critical Reynolds number is closer to a constant when scaled this way, but still varies somewhat at the lowest angles of attack. For the oscillatory flows in the following sections, we consider cases with $\alpha = 5^o$ at subcritical conditions ($Re = 300, 500$ and 1000), and with $\alpha = 15^o$ at both subcritical ($Re = 100$ and 200) and supercritical ($Re = 300, 400$ and 500) conditions. At $Re = 300$, we also consider a finer sweep of angle-of-attack from 5^o to 29^o.

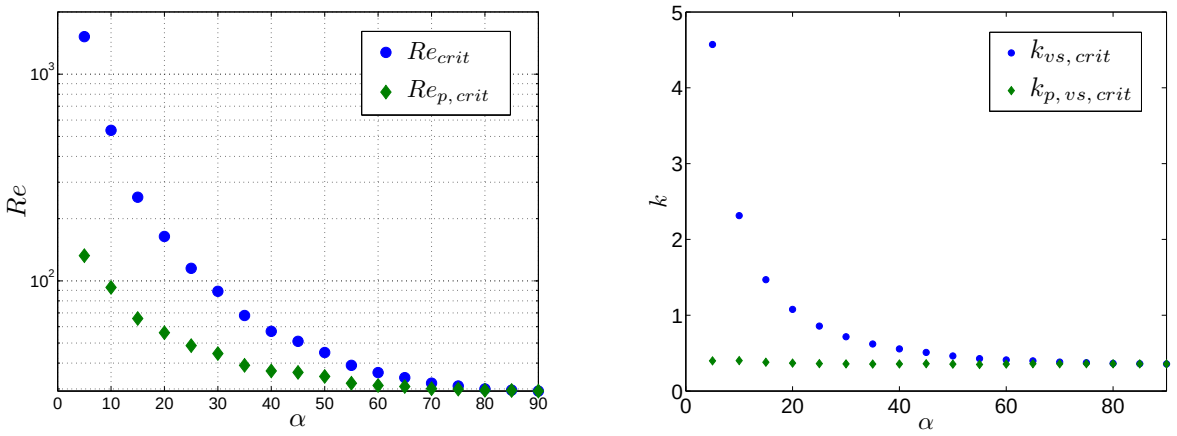

Figure 1. Critical Reynolds numbers ($Re_{\mathbf{crit}}$) and corresponding vortex shedding reduced frequencies ($k_{\mathbf{vs,\ crit}}$) at different angles of attack. The subscript p refers to quantities made dimensionless by the projected chord length, $c \sin \alpha$.

D. Inviscid Models

We compare our unsteady results to two models based on inviscid, incompressible (potential) flow theory. The first is Greenberg's model,[2] which is based on Theodorsen's function,[1] specialized to the case when the airfoil motion is combined with an unsteady freestream. In this model the flow is assumed to be attached, and the wake, which is formed at the trailing edge, convects with the same speed as the freestream velocity. The discrete vortex model (DVM) of Tchieu and Leonard[22] also assumes attached flow, but satisfies the Kutta condition with discrete vortices rather than a continuous distribution of vorticity. The vortices convect with the same speed as the freestream velocity, except for the nascent vortex (the vortex that is formed closest to the trailing edge) which moves at a speed that satisfies the Brown and Michael equation.[23] The DVM is a discrete version of the formula that was developed by Karman and Sears;[3] the formula for lift consists of three parts: a quasi-steady lift, an added-mass contribution, a contribution induced by the vorticity distribution in the wake. At high angle-of-attack, the real flow separates at the leading edge and we do not expect either model to accurately predict the forces.

III. Results

A. Response to Surging at Low Angle of Attack

We begin by examining surging for low angles of attack, $\alpha = 5^o$. For the flat plate, the flow is separated at the leading edge, but the separation bubble is narrow and, in the absence of oscillatory motion of the plate, is steady (subcritical) for the Reynolds numbers considered here. Figure 2 shows the amplitude and phase of the Fourier component of the fluctuating lift, denoted by $\hat{L}_k$, at the surging frequency, k, for small amplitude oscillations, $\sigma_x = 0.05$. The mean lift ($\bar{L}$) varies by less then 0.5% compared to the baseline ($\sigma_x = 0$) mean lift, L_0, and is not shown. The phase angle is computed relative to the imposed velocity fluctation with positive (negative) values indicating that lift leads (lags) the velocity.

Results from the inviscid models are also plotted in Figure 2, and, considering the large disparity in Re, there is reasonable agreement with the simulations. The computational results show additional oscillations in fluctuation amplitude that not predicted by the models. We believe these oscillations, which become more pronounced as the Reynolds number is increased, are related to leading edge separation on this flat-plate airfoil, and are harbingers of the behavior that occurs at higher α discussed in the next section. As expected, in the low frequency regime, $\hat{L}_\omega/L_0\sigma_x$ approaches 2 and ϕ approaches zero. In the high frequency regime, where the fluctuations are dominated by the added mass lift, $L_w/L_0\sigma_x$ has a nearly constant slope ($k/2$ for the potential models) and the phase of lift leads the velocity by a value approaching 90°, consistent with the added mass term being proportional to the acceleration. For the computational results, the slope is significantly higher than the potential flow limit, presumably due to large displacement effects associated with the low Reynolds numbers.

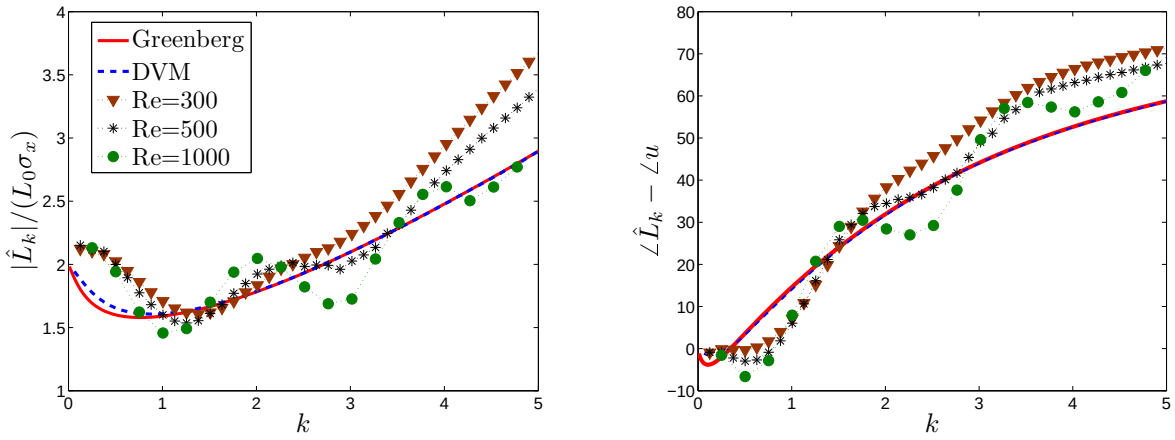

Figure 2. Amplitude (left) and phase (right) of fluctuating lift for $\alpha = 5$ and $\sigma_x = 0.05$.

In the intermediate region between the low and high frequencies, all three components of lift play a role in determining the amplitude and the phase of the fluctuating lift. The concave shape in the intermediate region can be interpreted with the aid of the DVM model. In the DVM, the trailing edge vortex is shed when its circulation reaches a maximum, and the amount of circulation it possess decreases as the surging frequency increases. This means that the trailing edge vortex is shed before it reaches its quasi-steady value, and the amplitude of total lift fluctuation should thus be smaller than the the value $L_{\omega,qs} + L_{\omega,am}$.

B. Response to Surging at High Angle of Attack

Deviations from the inviscid models becomes much more pronounced at higher angles of attack. Figure 3 shows the response of mean and fluctuating lift at a fixed $Re = 300$ for different values of α for a relatively small amplitude of surging, $\sigma_x = 0.2$. The inviscid models plotted in figure 2 are, when scaled by the baseline lift, independent of angle of attack and can directly compared to data in figure 3. This demonstrates the (not unexpected) inadequacy of inviscid theory to describe the dynamics for separated flow at high α.

Referring to figure 1, the critical angle-of-attack at $Re = 300$ is between 10° and 20°, and above this angle the natural flow is oscillatory at the vortex-shedding frequencies indicated by the colored vertical lines on the plot. For $\alpha = 5°$ and 10° (For which $Re < Re_{crit}$, the mean lift is very close to the baseline lift (L_0), consistent with the $O(\sigma_x^2)$ effect predicted by the inviscid theories. At angles for which $Re > Re_{crit}$, on the other hand, there is a significant increase in $\bar{L}$ that occurs over a range of frequencies. For the highest values of α, a strong peak in mean lift appears at a nearly constant k value which is distinct from the vortex shedding frequency. A detailed analysis of the flow shows that around the peak in mean lift, the entire flow (including the forces and the flow velocities in the wake) are resonating in a phase-locked manner. The wake instability is tuned, in these cases, to the surging frequency. This resonance is demonstrated in Figure 4 where a drag and lift polar at $\alpha = 29°$ is plotted for various values of k.

The fluctuating amplitude of lift in figure 3 shows that increasing α enhances or attenuates the fluctuations, depending on the reduced frequency. For frequencies in the range around $k = 0.4$ to $k = 0.7$, the fluctuating lift is high and increasing with increasing angle of attack. In the range $1.1 < k < 1.3$, there is a minimum in fluctuations, initially decreasing with increasing angle of attack.

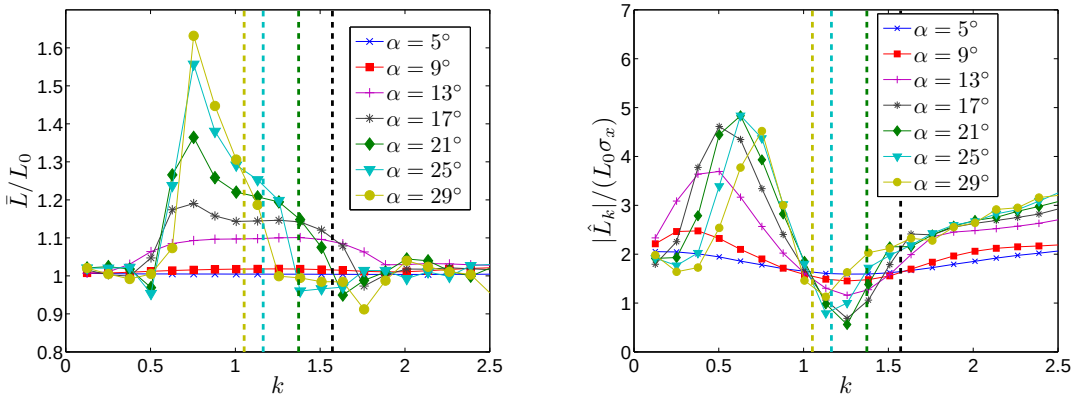

Figure 3. Mean lift (left) and lift fluctuation amplitude (right) at various angles, all with $Re = 300$ and $\sigma_x = 0.20$.

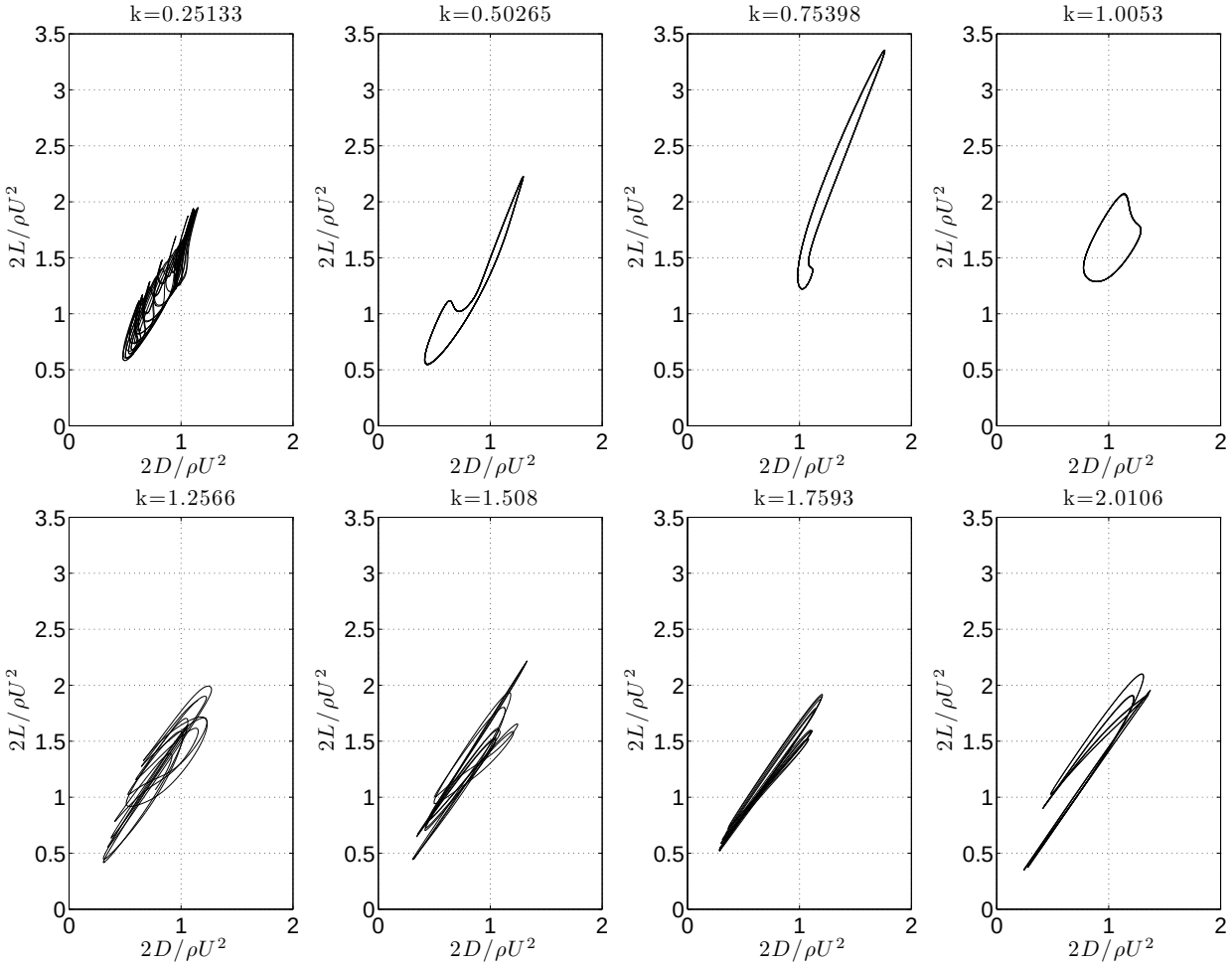

Figure 4. Lift-drag polar, at various reduced frequencies with $\alpha = 29°$, $Re = 300$, and $\sigma_x = 0.2$.

To further understand the origins of the range of k values associated with enhancement and suppression of lift fluctuations, we examine, in Figure 5 the amplitude and phase of lift fluctuations at a fixed angle of attack of $\alpha = 15^o$ over a range of Re, and include, for comparison, experimental results[13] at $Re = 57,000$. We note parenthetically that there is reasonable qualitative agreement between the computational results and the amplitude and phase of lift fluctuations measured in experiments at much higher Re.

For this angle, $Re_{crit} = 254$, and the vertical lines shows the natural vortex shedding frequency $k_{\rm VS}$ at $\sigma_x = 0$ for the supercritical values of Re. Note that these values are larger than those at Re_{crit}, i.e. $k_{\rm VS} > k_{\rm VS,crit}$, consistent with previous studies for bluff bodies.[24] Again we see a region with around $k = 0.5$ where the fluctuations are high and increasing with increasing Re, and a second region around $k = 1.3$ where fluctuations are minimal and decreasing with increasing Re. For $Re = 400$, the fluctuating magnitude of lift at $k = 0.5$ is more than twice the amplitude at $k = 0$ (the quasi-steady limit value) and at $k = 1.3$, it is less than half. For the supercritical Reynolds numbers, a second maximum in fluctuations occurs near the vortex shedding frequency, indicating a resonance with the wake instability

It is important to note that the k values where the first maximum and minimum fluctuations occur are not strongly related to the vortex shedding frequency, as is evident from figures 3 and 5. The peak fluctuation *levels* in the first maximum, however, grow with Reynolds number, at least in the low Reynolds number regime. This suggests that the origin of this effect is essentially different from wake instability.

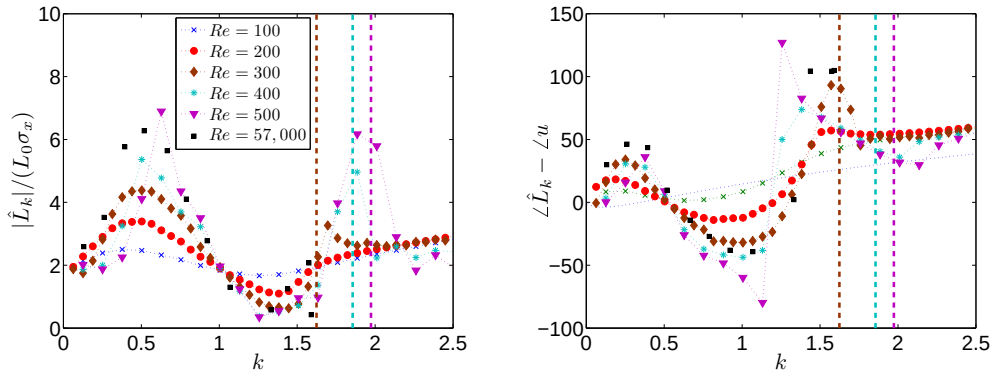

Figure 5. Amplitude (left) and phase (right) of lift fluctuations for various Re (including experiments[13]) at $\alpha = 15°$ and $\sigma_x = 0.05$.

To understand this behavior, we examine the instantaneous vorticity fields at $k = 0.50$ (figure 6) and $k = 1.26$ (figure 7). In each plot, the left and right columns show snapshots of the vorticity field (in the body fixed frame) when the velocity of the airfoil is at a maximum ($u = U(1+\sigma_x)$) and minimum ($u = U(1-\sigma_x)$), respectively. For $k = 0.50$, the left column shows a strong LEV forming above the top surface which, becomes more elongated and stronger as Re increases. At $k = 0.5$, the lift at maximum velocity is much higher than the quasi-steady case, and the augmented lift is attributed to the effect of LEV providing suction above the airfoil. On the other hand, at the minimum velocity (right column) the shear layer from the leading edge farther from the airfoil and the lift is reduced with the larger separation region. The incremental lift by the LEV is occurring with the maximum quasi-static lift, and lift reduction due to flow separation is occurring at the minimum velocity. Therefore the fluctuations are amplified. For $k = 1.26$ (figure 7) the situation is somewhat different. The LEV is still inducing low pressure regions above the airfoil; however, over the faster oscillation cycle, it only grows to a much smaller extent before it is shed during the retreating portion of the oscillation cycle. However, as this shed vortex advects, it remains close to the airfoil and produces a positive lift fluctuation during the retreating portion of the cycle, and thus offsets the negative quasi-steady component of lift and therefore *suppresses* the lift fluctuations.

This argument is strengthened by examining the phase of the instantaneous coefficient of lift, i.e., the phase of $\hat{C}_{L_k} = \frac{L}{\frac{1}{2}\rho u^2(t)c}$, which is shown in figure 8. In this way, we can exclude the fluctuations that are related to the quasi-static lift. Figure 8 plots the fluctuating amplitude and phase of $\hat{C}_{L_k}$, showing that $\hat{C}_{L_k}$ asymptotically reaches zero as k goes to zero. At $k = 0.5027$, the lift coefficient has maximum fluctuation

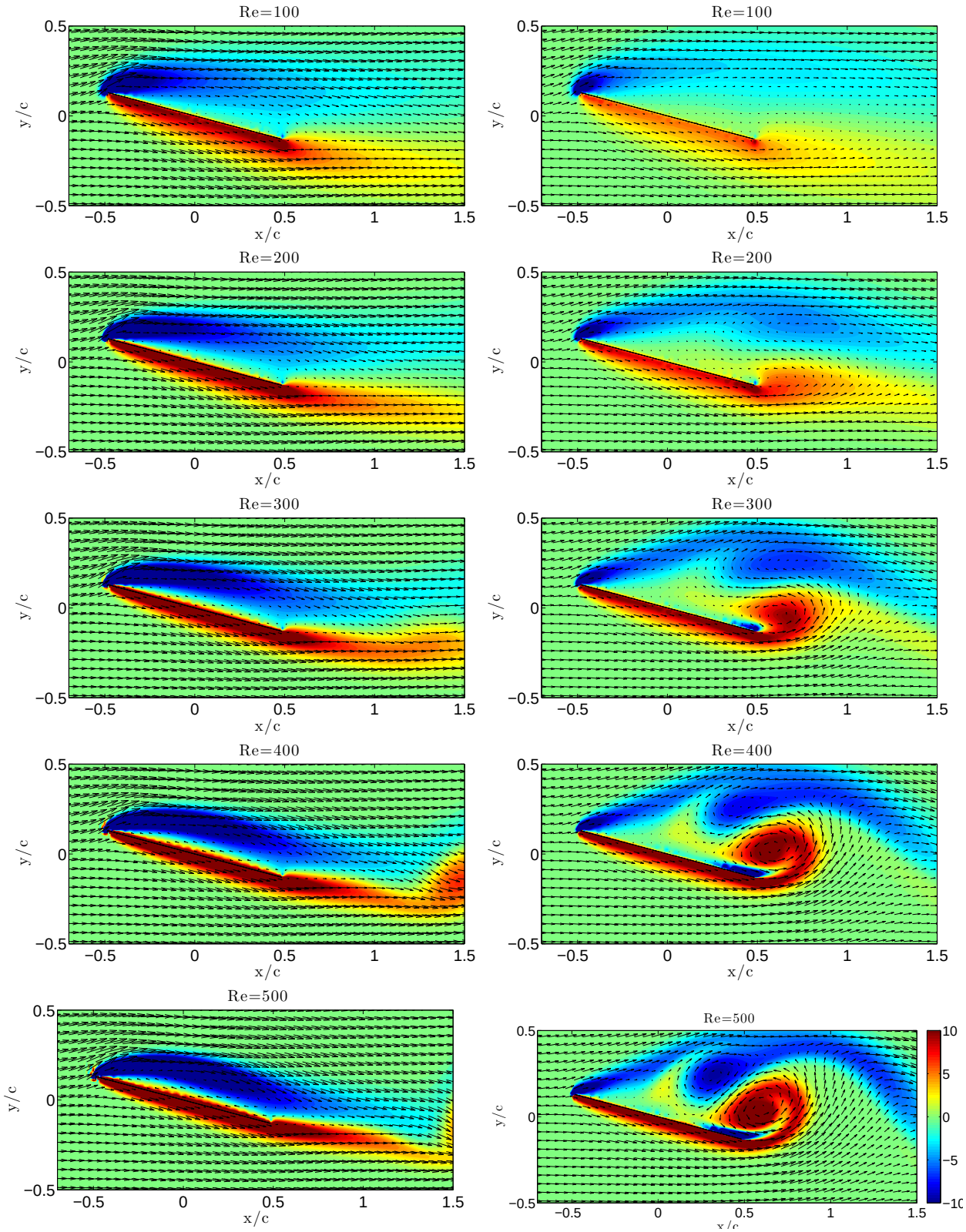

Figure 6. Snapshots of vorticity contours and velocity vectors at $\alpha = 15^\circ, \sigma_x = 0.02$ and $k = 0.5$. The left and right columns shows the field at the maximum $u = U(1 + \sigma_x)$ and minimum $u = U(1 - \sigma_x)$ speeds, respectively.

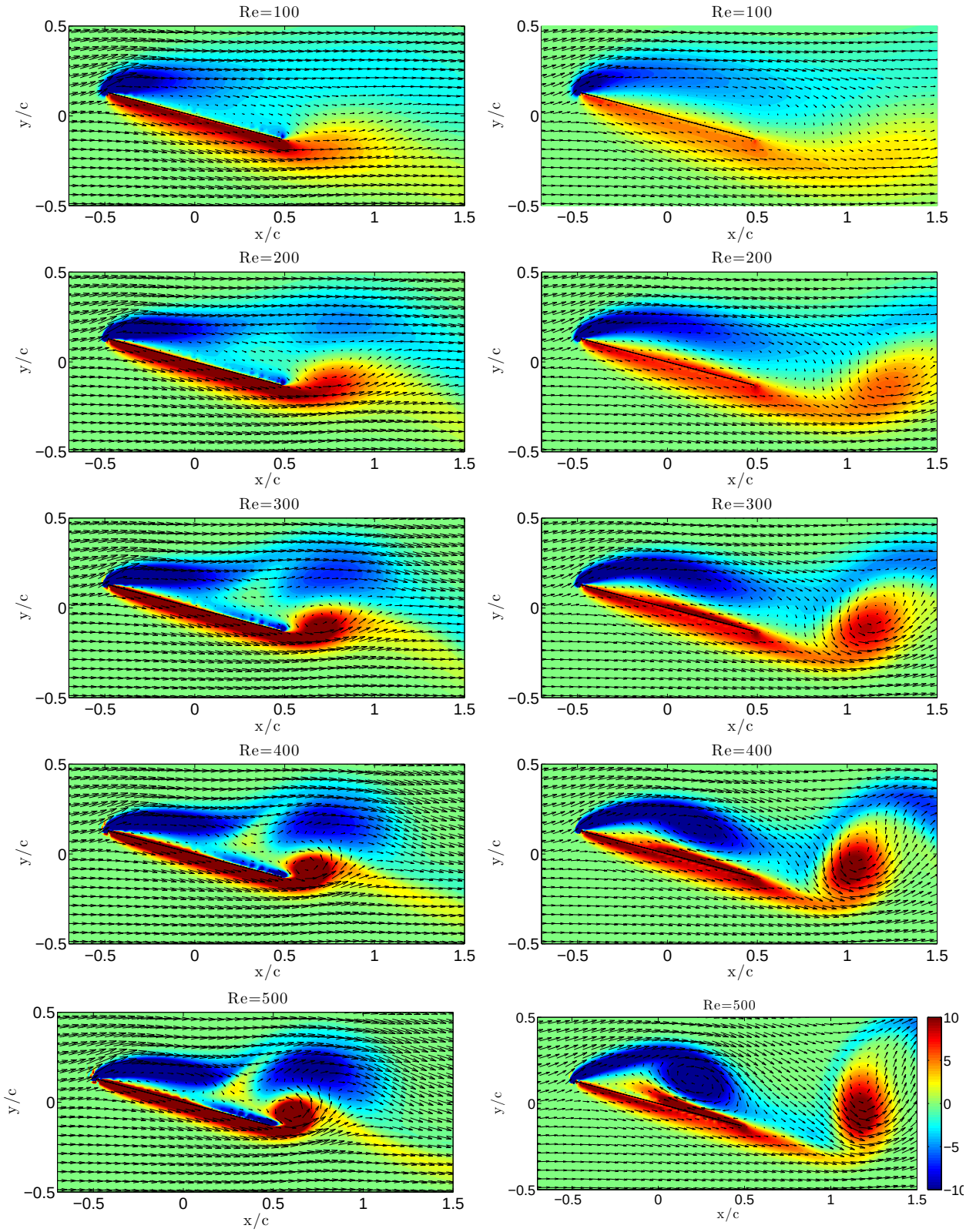

Figure 7. Same as figure 6 but at $k = 1.26$.

which occurs at the same phase of velocity ($\angle \hat{C}_{L_k} - \angle u = 0$), and at $k = 1.2566$ it has minimum fluctuation

with the opposite phase ($\angle \hat{C}_{L_k} - \angle u = 180°$).

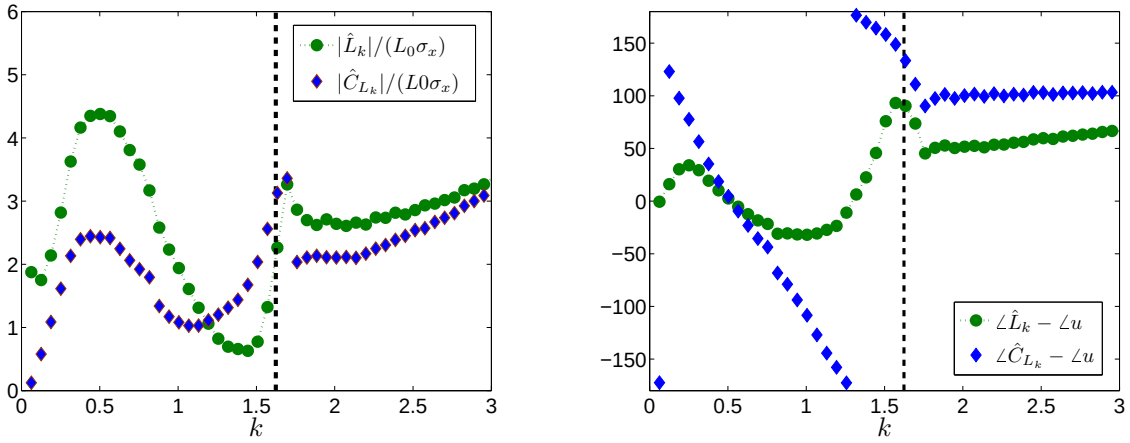

Figure 8. Amplitude (left) and phase (right) of the instantaneous coefficient of lift at $\alpha = 15°, Re = 300$ and $\sigma_x = 0.05$. (Fluctuating lift amplitude and phase at the same α, Re and σ_x plotted for comparison.)

Finally, lift fluctuations at $\alpha = 15°$ and $Re = 300$ are plotted in figure 9 for increasing values of amplitude, σ_x. The behavior is similar through $\sigma_x = 0.4$, but as σ_x increases there is a growing asymmetry between the fluctuation enhancement around $k = 0.5$ and the suppression near $k = 1.26$. When $\sigma_x > 0.4$, lift fluctuations are no longer proportional to σ_x and shows nonlinear behavior.

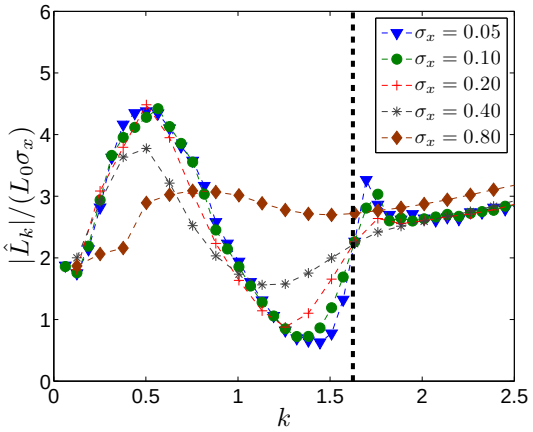

Figure 9. Fluctuating lift amplitude at $Re = 300$ and $\alpha = 15°$

Next, we look at the flow response at various σ_x, which is equivalent to varying St_A since $St_A = \sigma_x/\pi$ for our case. Figure 10 plots the lift fluctuation and mean lift-to-drag ratio at various surging amplitude. The mean lift-to-drag ratio, also increases with higher surging amplitude, and in terms of achieving high lift-to-drag ratio, it increases the performance of the airfoil. The data presented are not sufficient to conclude that $0.2 < St_A < 0.4$ is the optimal range for flying, since the largest σ_x corresponds to $St_A = 0.2546$, however, the results show that the mean lift-to-drag increase at nearly all reduced frequency as St_A gets closer to this range. St_c, on the other hand, seems to be the principal parameter that determines the behavior of lift fluctuation, which we have shown similar results by expanding α, Re and σ_x.

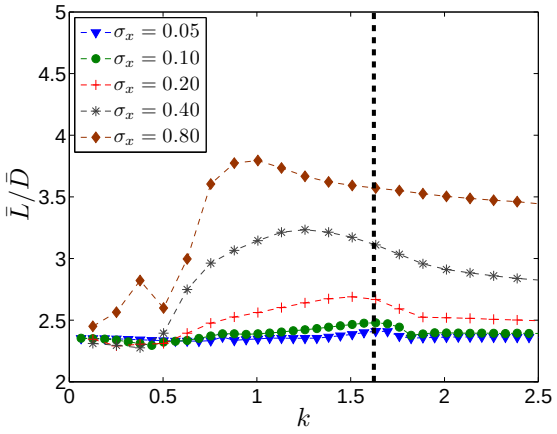

Figure 10. Mean lift-to-drag Ratio (right) at $Re = 300$ and $\alpha = 15°$

C. Response to Plunging

The lift fluctuations associated with plunging are now evaluated at $\alpha = 5^o$ and $\alpha = 15^o$. In figure 11, we compare the amplitude and phase of the fluctuations between surge with $\sigma_x = 0.05$ and plunge with $\sigma_y = 0.05$ for $Re = 300$. As for the case of surging, the response at $\alpha = 5^o$ corresponds reasonably well with the inviscid flow models. The generally higher fluctuation levels of plunging can be understood by noting that unlike surging, plunging involves oscillations in both speed and effective angle of attack, α_e, given by

$$\alpha_e = \alpha + \tan^{-1}\left(\frac{\sigma_y U \sin\omega t}{U}\right) = \alpha + \tan^{-1}(\sigma_y \sin\omega t). \tag{3}$$

For $\alpha = 15^o$, similar maximum and minimum fluctuations occur at frequencies close to those found in the surging case, but, again, at all angles of attack, the fluctuation levels are much higher in plunging motion. The variation of α_e is bounded by σ_y, and if σ_y is large, the response shows strong nonlinear effects. Figure 13 shows lift fluctuations and mean lift-to-drag ratio as a function of σ_y. The response becomes nonlinear at a smaller value of σ_y around 0.2, but the mean lift-to-drag ratio shows comparable levels and of enhancement and generally similar trends with reduced frequency as the surging case.

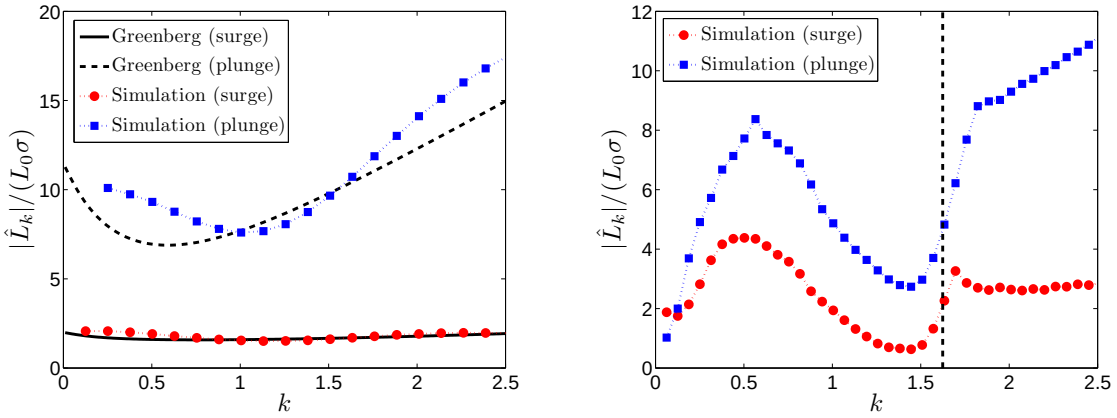

Figure 11. Amplitude of lift fluctuations for $\alpha = 5^o$ (left) and $\alpha = 15^o$ (right) at $Re = 300$ for surging with $\sigma_x = 0.05$ and plunging with $\sigma_y = 0.05$.

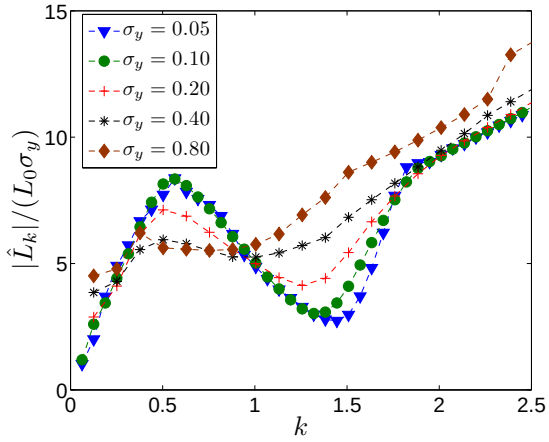

Figure 12. Fluctuating lift amplitude at $Re = 300$ and $\alpha = 15°$.

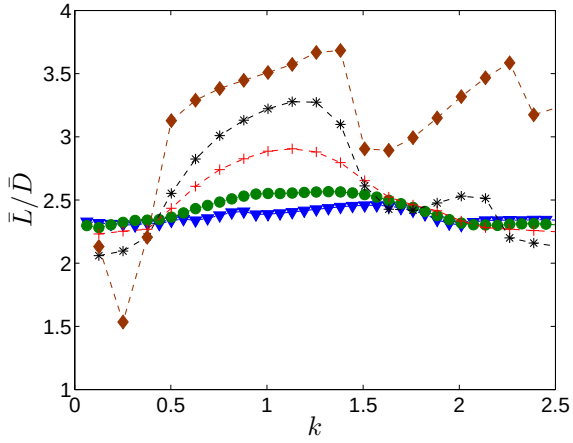

Figure 13. Mean lift-to-drag ratio at $Re = 300$ and $\alpha = 15°$.

D. Energy Extraction in Gusting Flows

Langelaan[4] considers the airfoil as a point mass and evaluates the power (P) supplied or extracted by the airfoil in an unsteady stream. Using our notation and the harmonic surging and plunging motion given by equation (1), the period-averaged power is, in the absence of thrust,

$$\frac{Pm}{\frac{1}{2}\rho c U^3} = -\frac{1}{T}\int_t^{t+T}\Big(\left(1+\sigma_x \sin\left(2ktU/c\right)\right)C_D + \sigma_y \sin\left(2ktU/c+\theta\right)C_L\Big)dt, \tag{4}$$

where m is the mass of the airfoil. Relative to the baseline case of steady motion with speed U, the percent change in required power is given by

$$\frac{P-P_0}{P_0} = -\frac{\bar{C}_D - \bar{C}_{D_0}}{\bar{C}_{D_0}} - \frac{1}{T}\int_t^{t+T}\left(\sigma_x \sin\left(2ktU/c\right)\frac{C_D}{\bar{C}_{D_0}} + \sigma_y \sin\left(2ktU/c+\theta\right)\frac{C_L}{\bar{C}_{D_0}}\right)dt. \tag{5}$$

The first term on the right hand side is generally negative (meaning that the surging/plunging airfoil requires more power than the steady one) for the cases we have considered. Useful energy extraction from the gust would come from a lag between surge and drag (or plunge and lift) between -90^o and 90^o. Figure 14 shows the percent change in power for surging and plunging motions with low values of σ_x and σ_y, respectively for the subcritical flow at $Re = 200$. The results show that plunging leads to larger differences

in power from the baseline case than surging, which is related to the generally higher fluctuation levels across all frequencies. These results show that the optimal frequency ranges for energy extraction occur near the $k = 0.5$ peak where fluctuating lift/drag is maximized, and in phase with the surging/plunging velocity. Similarly, the penalty occurs for values around the k values associated with the minimal fluctuations in lift/drag. The maximum value of power savings is very modest in figure 14, about 4%. In companion experiments,[13] combined surging and plunging motion with $\sigma_x = \sigma_y = 0.05$ yielded 40%.[13] We believe the large difference is associated with the low Reynolds number; for example the much larger baseline drag at $Re = 200$ compared to $Re = 57,000$ penalizes the plunging term in equation 5. Our future research will be aimed investigating energy extraction in greater detail at higher Reynolds number.

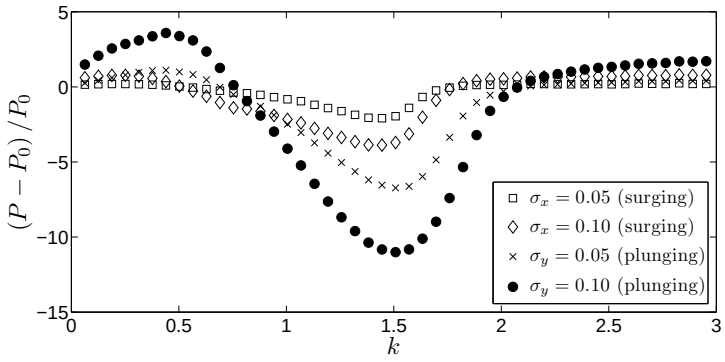

Figure 14. Energy gain (%) for equivalent surging and plunging motions compared to P_0. ($Re = 200, \alpha = 15°$)

IV. Conclusions

We have investigated the flow structure of mean and fluctuating lift associated with surging and plunging motion of a wing superposed on a steady flow. We have concentrated on the low Reynolds number regime straddling the critical Reynolds number where the baseline flow first displays wake instabilities and vortex shedding. We varied the surging and plunging motion over a wide range of reduced frequency and amplitude. For relatively low angles of attack, the results are generally consistent with inviscid potential flow models, whereas at high angle of attack, separated flow has a significant impact on the dynamics which show a richer dependence on reduced frequency than the inviscid models.

The most interesting feature is that there exists a range of k values for which lift fluctuations are maximized and a region of k values where lift fluctuations are minimized. For the surging case, there was typically a doubling of the quasi-static lift fluctuations at the maximum and a 50% reduction at the minimum. This behavior does not appear to be fundamentally related to wake instability, as the associated frequencies show no significant dependence on Reynolds number, angle of attack, and amplitude, at least up through about 40% oscillations. In particular, both subcritical and supercritical flows show the same dynamics at low amplitude of oscillation. Supercritical flows, especially at relatively large surge/plunge amplitudes, give rise to more a more complex resonant response with lock-on to vortex shedding and correspondingly large changes in mean lift, drag, and lift-to-drag ratio. These frequencies associated with maximal and minimal lift fluctuations were similar for both surging and plunging motions, but the surging cases have been analyzed in greater detail.

The results show that at both frequencies that minimize and maximize lift fluctuations, lift was nearly in phase with the freestream velocity. At the maximum in fluctuations, contributions from the shed vorticity (in both the separated region above the airfoil and from the trailing edge) lead to forces that are in phase with the quasi-static component of the lift, whereas at the minimum in fluctuations, these contributions are out of phase, and nearly cancel, the quasi-static component of lift. Analysis of the flow structures in the surging case show that the main contributor to this process appears to be the LEV that forms during the advancing portion of the surge cycle. At the lower k value associated with maximal fluctuations, this

LEV attains an extent about equal to the chord, whereas at the higher k value associated with minimal fluctuations, it is less than half a chord in extent. At the higher frequency, this vortex is shed during the retreating portion of the surge cycle, but then advects close to the plate after it is shed, such that it still produces a positive lift fluctuation during the retreating portion of the surge cycle when the quasi-static lift contribution is negative. The cancellation thus results in minimization of fluctuations.

Based on this observation, we suggest that the representative k value for maximizing lift fluctuations is associated with the (inverse of the) vortex formation time beyond which an LEV is shed (typically measured for an impulsively-started wing). Taking $k \approx 0.5$ for the maximum, the characteristic period is $TU/c = 6.28$, which is similar to the low-Reynolds value of the "universal" vortex formation number reported by Chen et al.[25] Finally, the frequency associated with the maximum lift/drag fluctuations for surging/plunging was found to minimize the power required to propel the airfoil, owing to the fact that drag/lift fluctuations occur in phase with the freestream velocity at this frequency.

Acknowledgments

This work was supported by the Air Force Office of Scientific Research (FA950-09-1-0189).

References

[1]Theodorsen, T., "General theory of aerodynamic instability and the mechanism of flutter," NACA Rep. 496, 1935.

[2]Greenberg, J., "Airfoil in sinusoidal motion in a pulsating stream," NACA TN 1326, 1947.

[3]Von Karman, T. and Sears, W., "Airfoil theory for non-uniform motion," *Journal of Aeronautical Sciences*, Vol. 5, No. 10, 1938, pp. 379–390.

[4]Langelaan, J. and Bramesfeld, G., "Gust energy extraction for mini and micro uninhabited aerial vehicles," *Journal of guidance, control, and dynamics*, Vol. 32, No. 2, 2009, pp. 464–473.

[5]Lissaman, P., "Wind energy extraction by birds and flight vehicles," *AIAA Paper 2005-241, 43rd AIAA Aerospace Sciences Meeting and Exhibit*, Reno, Nevada, USA, Jan 2005.

[6]Denny, M., "Dynamic soaring: aerodynamics for albatrosses," *European Journal of Physics*, Vol. 30, 2009, pp. 75–84.

[7]Wang, Z., "Dissecting insect flight," *Annu. Rev. Fluid Mech.*, Vol. 37, 2005, pp. 183–210.

[8]Ellington, C., Van Den Berg, C., Willmott, A., and Thomas, A., "Leading-edge vortices in insect flight," *Nature*, 1996.

[9]Dickinson, M. and Gotz, K., "Unsteady aerodynamic performance of model wings at low Reynolds numbers," *Journal of Experimental Biology*, Vol. 174, No. 1, 1993, pp. 45–64.

[10]Taylor, G., Nudds, R., and Thomas, A., "Flying and swimming animals cruise at a Strouhal number tuned for high power efficiency," *Nature*, Vol. 425, No. 6959, 2003, pp. 707–711.

[11]Triantafyllou, M., Triantafyllou, G., and Gopalkrishnan, R., "Wake mechanics for thrust generation in oscillating foils," *Physics of Fluids A: Fluid Dynamics*, Vol. 3, 1991, pp. 2835.

[12]Triantafyllou, M., Triantafyllou, G., and Yue, D., "Hydrodynamics of fishlike swimming," *Annu. Rev. Fluid Mech.*, Vol. 32, No. 1, 2000, pp. 33–53.

[13]Williams, D., Kerstens, W., and Quach, V., "Drag-power measurements of a plunging wing in an oscillating freestream," *AIAA Paper 2011-3255, 41st AIAA Fluid Dynamics Conference and Exhibit*, Honolulu, Hawaii, USA, Jun 2011.

[14]Jones, K., Dohring, C., and Platzer, M., "Modelling thrust generation of a two-dimensional heaving airfoil in a viscous flow," *J. Fluid Mech.*, Vol. 492, 2003, pp. 339–362.

[15]Jones, K., Dohring, C., and Platzer, M., "Wake structures behind plunging airfoils: a comparison of numerical and experimental results," *AIAA Paper 1996-78, 34 th AIAA Aerospace Sciences Meeting and Exhibit*, Reno, Nevada, USA, Jan 1996.

[16]Andro, J. and Jacquin, L., "Frequency effects on the aerodynamic mechanisms of a heaving airfoil in a forward flight configuration," *Aerospace Science and Technology*, Vol. 13, No. 1, 2009, pp. 71–80.

[17]Cleaver, D., Wang, Z., Gursul, I., and Visbal, M., "Lift Enhancement by Means of Small-Amplitude Airfoil Oscillations at Low Reynolds Numbers," *AIAA journal*, Vol. 49, No. 9, 2011, pp. 2018–2033.

[18]Cleaver, D., Wang, Z., and Gursul, I., "Bifurcating flows of plunging aerofoils at high Strouhal numbers," *J. Fluid Mech.*, Vol. 1, No. 1, 2012, pp. 1–28.

[19]Colonius, T. and Taira, K., "A fast immersed boundary method using a nullspace approach and multi-domain far-field boundary conditions," *Computer Methods in Applied Mechanics and Engineering*, Vol. 197, No. 25, 2008, pp. 2131–2146.

[20]Taira, K. and Colonius, T., "The immersed boundary method: a projection approach," *Journal of Computational Physics*, Vol. 225, No. 2, 2007, pp. 2118–2137.

[21]Fage, A. and Johansen, F., "On the flow of air behind an inclined flat plate of infinite span," *Proceedings of the Royal Society of London. Series A, Containing Papers of a Mathematical and Physical Character*, Vol. 116, No. 773, 1927, pp. 170–197.

[22]Tchieu, A. and Leonard, A., "A discrete-vortex model for the arbitrary motion of a thin airfoil with fluidic control," *Journal of Fluids and Structures*, Vol. 27, 2011, pp. 680–693.

[23]Brown, C. and Michael, W., "Effect of leading edge separation on the lift of a delta wing," *J. Aero. Sci*, Vol. 21, No. 10, 1954, pp. 690–694.

[24]Sreenivasan, K., Strykowski, P., and Olinger, D., "Hopf bifurcation, Landau equation, and vortex shedding behind circular cylinders," *Forum on Unsteady Flow Separation*, Vol. 1, 1987, pp. 1–13.

[25]Chen, K., Colonius, T., and Taira, K., "The leading-edge vortex and quasisteady vortex shedding on an accelerating plate," *Physics of fluids*, Vol. 22, No. 3, 2010.